JOURNAL OF THERMOPHYSICS AND HEAT TRANSFER
Vol. 8, No. 3, July–Sept. 1994

Measurements of Temperature and Seed Atom Density in High-Speed MHD Flows

Leslie E. Bauman,* Weishun Wang,† John C. Luthe,‡ and R. Arun Kumar§
Mississippi State University, Mississippi State, Mississippi 39762

Emission absorption measurements of temperature, potassium seed atom density, and electron conductivity have been demonstrated in the high-speed, turbulent coal-fired flow of a simulated MHD channel. A two-beam optical system provides coincident exposures of transmitted lamp and emission-only signals with a time resolution of one-half ms. Multiwavelength detection allows for optimization of the measurement wavelengths for a two-wavelength analysis that eliminates error due to ash/slag particle extinction and emission. Previous measurements with single beam, 1 ms temporally separated measurements showed large standard deviations due to fluctuations in flow parameters between the two noncoincident exposures. Comparison of the two types of measurements for nominally the same flow conditions reveals the considerable improvement in measurement uncertainty with the two-beam optical system.

Nomenclature

B = Planck blackbody function
C_2 = Planck second blackbody constant
E = particle extinction-to-absorption ratio
E_i = ionization energy
e = electron charge
g = statistical weight factor
h = Planck constant
I = light intensity
J_λ = in-scatter light intensity at wavelength λ
k = Boltzmann constant
L = total optical path length across the flow
m = mass, subscripts for electron e, foreign atom f, and potassium atom K
n = number density with subscripts for seed atom K, seed ion i, electron e, and standard temperature and pressure s
P = pressure, subscript for standard s
T = temperature with subscripts for core flow c, standard s, wall w, and path position x
x = optical path position
z = particle temperature to gas temperature Planck ratio
α_λ = atomic resonance line absorption coefficient
η = particle absorption coefficient
λ = wavelength or subscript denoting wavelength
μ_e = electron mobility
σ_e = electron conductivity
σ_λ = potassium absorption coefficient per atom
τ = optical depth
Φ = gas-to-lamp Planck blackbody intensity ratio
Ω_p = particle cloud albedo

Presented as Paper 93-3215 at the AIAA 24th Plasmadynamics and Lasers Conference, Orlando, FL, July 6–9, 1993; received Aug. 12, 1993; revision received Feb. 7, 1994; accepted for publication Feb. 8, 1994.

*Senior Research Scientist and Professor of Physics and Chemistry, Diagnostic Instrumentation and Analysis Laboratory, P.O. Box MM. Member AIAA.

†Research Scientist, Diagnostic Instrumentation and Analysis Laboratory, P.O. Box MM.

‡Research Scientist II, Diagnostic Instrumentation and Analysis Laboratory, P.O. Box MM.

§Research Engineer II, Diagnostic Instrumentation and Analysis Laboratory, P.O. Box MM.

Introduction

ACCURATE measurements of temperature, seed atom density, and electrical conductivity are crucial for evaluating and monitoring MHD combustion flows. A multiwavelength potassium emission absorption system (PEAS) has been successfully employed for such measurements for numerous field tests in the subsonic diffuser test sections of two coal-fired MHD facilities, the Coal-Fired Flow Facility (CFFF) at the University of Tennessee Space Institute, and the Component Development and Integration Facility (CDIF) in Butte, Montana.[1] The diffuser test sections provide the transition between the supersonic MHD channel and the radiant boiler. With optical access provided to the aerodynamic duct of the CFFF, a test section designed to simulate an MHD channel, emission absorption measurements of temperature and seed density have been made for the first time in the upstream of a prototype coal-fired MHD facility.[2] With large fluctuations in the flow properties at this location, it provides an extreme challenge for nonintrusive diagnostic measurements.[3]

Three basic signals are needed for emission absorption measurements: 1) emission, 2) transmitted lamp, and 3) a reference lamp. The reference lamp signal can be collected prior to the test; separating the other two signals is challenging and the method employed determines the system performance. Basic schemes depend upon either temporal or spatial separation. Previous reported techniques from other researchers with the potential of high-speed time resolution include a knife wedge method[4] and a light polarization technique.[5] Both methods are impractical for measurements on large-scale facilities because both require careful optical alignment and are especially sensitive to any vibration that may move the knife wedge or the polarizer. A high-speed technique using individual photodiode detectors positioned on and closely off a white light image provided insensitivity to vibration and simple alignment.[6] However, by using a line filter for spectral separation, the technique did not provide the multiwavelength signals necessary for accurate measurement in coal-fired MHD flows.

Standard operation of the PEAS instrument relies upon temporal separation of the signals. Large standard deviations in the measurement uncertainties at this location led to the design and construction of a two-beam, spatially separated optical scheme for the instrument. The new scheme provided much improved measurements. This article briefly compares the two different signal separation schemes, presents typical

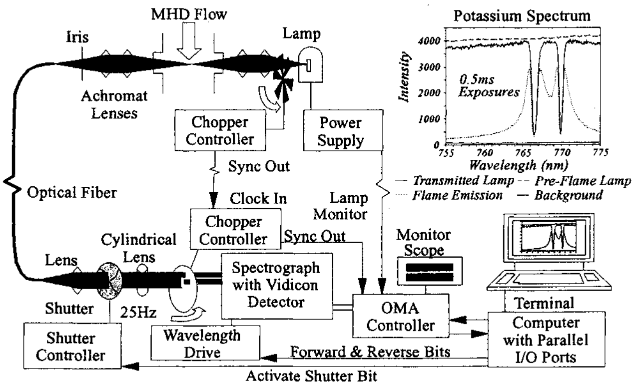

Fig. 1 Multiwavelength potassium emission absorption system diagram. Synchronized optical choppers separated transmitted lamp and emission-only signals on two halves of a vidicon detector.

field test results, and demonstrates the ability to provide accurate measurements on high-speed, turbulent flows.

Instrument

PEAS is a multiwavelength spectroscopic system developed for measurements of temperature, seed atom density, and electron density or conductivity in coal-fired MHD flows. The instrument provides direct measures of the average temperature and seed atom density, and from these measurements it calculates the electron number density and electron conductivity by assuming ionization equilibrium and an electron collision frequency model. These calculations are presented briefly below.

In its typical configuration, the system uses a system of synchronized optical choppers and a vidicon multichannel detector to provide quasi-time-resolved, spatially coincident emission absorption signals.[7] The typical optical setup is diagrammed in Fig. 1. The emission absorption signals are recorded on separate tracks of the vidicon detector—a track consists of 500 channels of data. Each signal is an exposure of 0.5 ms and the signals are separated by 1 ms. It is important that the instrument provides time-resolved spectra because of the nonlinear relationship between the intensities and the atomic density. Each channel of data corresponds to approximately 0.06 nm, but with the inherent bleed of the vidicon detector of about three channels the instrument resolution is about 0.2 nm, sufficient to resolve the broad potassium lines. A recorded reference lamp signal from the tungsten strip lamp provides the instrument response calibration and a potassium spectral lamp is used to calibrate the wavelength scale.

With high seed loading of potassium and long optical path length, the potassium doublet resonance line in seeded MHD flows is very broad and deeply self-reversed so that spectrally resolved measurements are made in the line wings to avoid errors due to the cooler boundary layers.[8] In addition, two wavelength analysis cancels errors due to the broadband effects of the ash/slag particle cloud.[9] The multiwavelength nature of the instrument allows for optimization of the choice of measurement wavelength and analysis techniques depending upon the flow dimensions and potassium loading.

Emission Absorption Measurements

Radiative Transfer Equation

At a resonance line in a high-temperature flow, the transmitted lamp signal is a line-of-sight integral across the flow as

$$I_\lambda(L) = e^{-\tau_L}\int_0^L (\alpha_\lambda + z\eta)B_\lambda(T_x)e^{\tau_x}\,dx + I(0)e^{-\tau_L} + J_\lambda \tag{1}$$

where the optical depth at position x is

$$\tau_x = \int_0^x (\alpha_\lambda + \eta E)\,dx' \tag{2}$$

Here, $I(0)$ is the incident lamp signal, and $I(L)$ is the outgoing light from the flow at a path length of L. The particle inscatter term is included as J. The emission only intensity is found by setting $I(0)$ to zero. The atomic absorption coefficient α_λ is a function of x through its linear dependence upon atomic density and its dependence on temperature and total density through line broadening mechanisms.

Broadband particle effects are included as η, E, and the ratio of Planck blackbody functions at the particle temperature to the gas temperature at x as $z = B_\lambda(T_p)/B_\lambda(T_x)$. The particle cloud albedo is related to E as $\Omega_p = (E - 1)/E$.

Constant Property Flows

The potassium D-line emission spectra on seeded MHD flows are deeply self-reversed due to the cooler boundary layers; however, the boundary layers are thin and the spectra in the line wings can be well approximated as that of a constant property flow as

$$I_{L+G} = [(\alpha_\lambda + z\eta)/(\alpha_\lambda + \eta E)]B_\lambda(T_G)(1 - e^{-\tau_\lambda}) + I_L e^{-\tau_\lambda} + J_\lambda \tag{3}$$

where the emission from the hot gases I_G is the first term, and the second term is the transmitted lamp signal, i.e., the incident lamp at $x = 0$ reduced by the total optical depth. The total optical depth can be calculated as

$$\tau_\lambda = (\alpha_\lambda + \eta E)L = \ln[I_L/(I_{L+G} - I_G)] \tag{4}$$

With a temporal separation scheme, there is always a time delay between the emission signal and the transmitted lamp signal. Changes in atomic density, particle loading, or flame temperature between collection of the signals will introduce error into the measurement.

Temperature Determination

The gas temperature is calculated by a modified line reversal technique. The Planck blackbody function ratio of gas temperature to reference lamp temperature at a single wavelength is

$$\Phi_\lambda = \frac{B_\lambda(T_G)}{B_\lambda(T_L)} = \frac{I_G}{I_L - I_{L+G} + I_G} \tag{5}$$

with the gas temperature then found as

$$\frac{1}{T_G} = \frac{1}{T_L} + \frac{\lambda}{C_2}\ln(\Phi) \tag{6}$$

Temperatures found by single wavelength measurements will be in error due to particle effects, misalignments, dirty windows, etc.[10] These broadband effects can be eliminated by determining Φ from two-wavelength measurements as

$$\Phi_{2\lambda} = [(\tau_{\lambda_1}\Phi_{\lambda_1} - \tau_{\lambda_2}\Phi_{\lambda_2})/(\tau_{\lambda_1} - \tau_{\lambda_2})] \tag{7}$$

Potassium Number Density Measurement

The emitter number density, in this case neutral potassium atom number density, is found as

$$n_K = [(\tau_{\lambda_1} - \tau_{\lambda_2})/(\sigma_{\lambda_1} - \sigma_{\lambda_2})] \tag{8}$$

where $\sigma_\lambda = \alpha_\lambda/n_K$ is the absorption coefficient per atom. An experimentally determined power law profile matched to a Voigt profile on the blue wing of the D_2 line was used for calculating the atomic absorption coefficient.[11] The accuracy of the number density determination will be limited by the knowledge of the absorption coefficient.

Electron Density Determination

The electron density can be found by assuming that the K^+ ion density n_{K^+} is equal to the electron density n_e, and is related to the seed atom density n_K through a function of temperature as given by the Saha equation for ionization equilibrium:

$$\frac{n_e n_{K+}}{n_K} = \frac{(2\pi m_e kT)^{3/2}}{h^3} \frac{2g_i}{g_0} \exp\left(-\frac{E_i}{kT}\right) \tag{9}$$

where the statistical weight ratio g_i/g_0 is $\frac{1}{2}$ for the alkali metals, and E_i is the potassium first ionization energy.

Electron Conductivity Determination

With an electron mobility model the electron conductivity is calculated from the electron density as

$$\sigma_e = e\mu_e n_e \tag{10}$$

For these experiments on the CFFF aerodynamic duct, thermodynamic equilibrium calculations were used to determine the neutral and ion species concentrations at standard operating conditions, with the seed loading varied from 0.6 to 1.8% potassium by weight in order to cover the expected operating envelope of MHD channels. The electron mobility was determined by the method presented by Frost,[12] with a numerical integration over the Maxwellian distribution of electron velocities including both electron-neutral and electron-ion collision frequencies. Example mobility results are shown in Fig. 2.

Experiment Results

Figure 3 plots typical emission absorption measurements in the CFFF diffuser using temporal separation of the signals. The measurements are made from individual one-half-ms exposures taken every 1 s. Lines showing plus and minus one measurement standard deviation are shown dotted, whereas the solid line shows the average values for sets of 50 measurements. The standard deviations represent the instrument uncertainty combined with the true fluctuations in the flow. The standard deviations are about double that for the best instrument uncertainty as found experimentally on a stable bench-top flame. This indicates a reasonably small and acceptable instrument uncertainty for measurements in the diffuser.

Measurements in the optical test section of the aerodynamic duct shown below are from the LMF5 series tests on CFFF facility with Rosebud coal and a nominal primary stoichiometry of 0.85. The flow diameter is 12 cm and the measurement port is approximately 3 pipe diameters down from the coal-fired combustor. The flow pressure is estimated to be about 2 atm at the optical port location and the flow velocity is quite high (>1000 m/s). The flow is expected to be much more turbulent and to show greater fluctuations at this location closer to the coal-fired combustor as compared to the diffuser.

The optical access is limited to 1-in. windows with a large f number of 9. This limited access combined with a limited space for optics on rails in front of the windows, led to the choice of a collimated optical arrangement for the first measurements on the aerodynamic duct as shown in Fig. 4. Figure 5 shows measurements at the CFFF aerodynamic duct for temporal signal separation.

In spite of the noisy measurement results in the aerodynamic duct, the PEAS instrument was able to provide useful measurements as shown in Fig. 6 for measurements of potassium number density at differing seed loading during the LMF5-F test. The general trends agree with the planned facility seed loading changes.

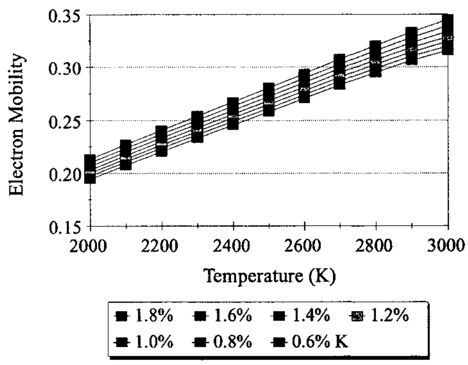

Fig. 2 Electron mobility calculations for the aerodynamic duct at a pressure of 2 atm.

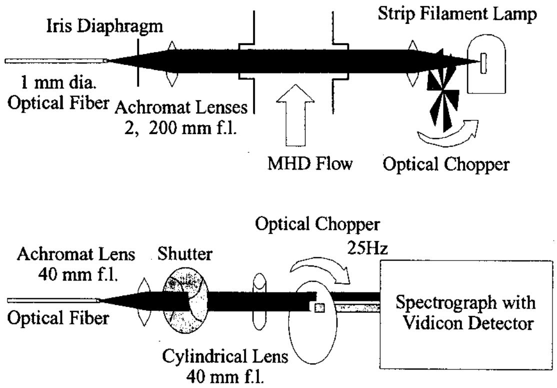

Fig. 4 Optical arrangement for spatially coincident, temporally separate emission absorption signals.

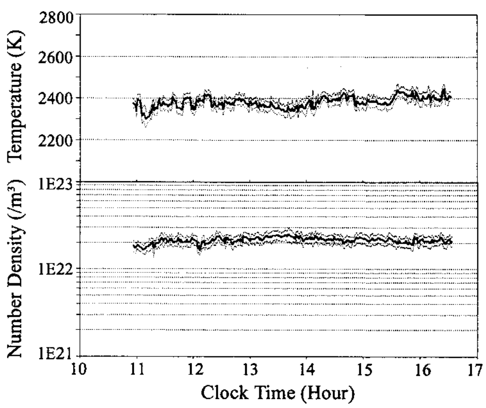

Fig. 3 Typical measurements of temperature and potassium atom number density in the diffuser of the CFFF.

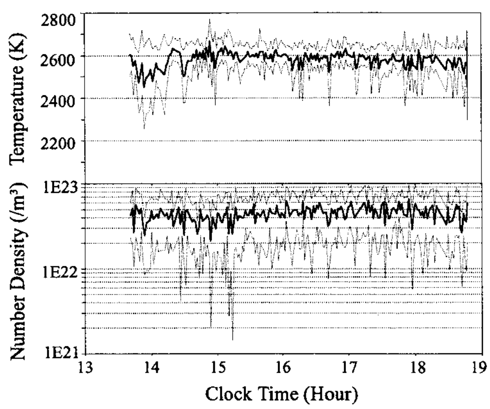

Fig. 5 Measurements of temperature and potassium atom number density in the aerodynamic duct of the CFFF for the LMF5-C test.

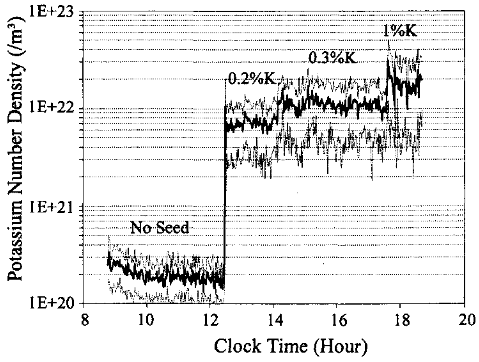

Fig. 6 Potassium atom number density measurements in the aerodynamic duct of the CFFF for the LMF5-F test.

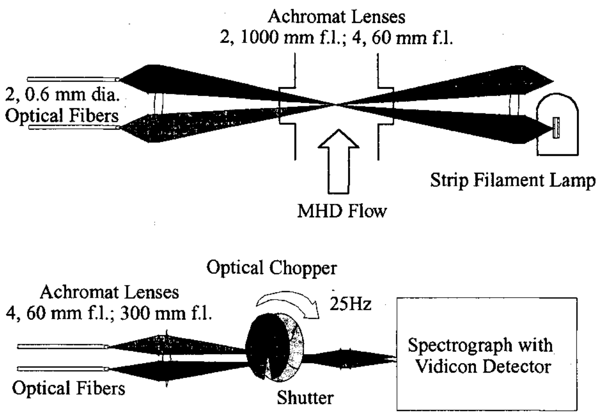

Fig. 7 Potassium emission absorption system diagram for spatially separate, temporally coincident signal collection.

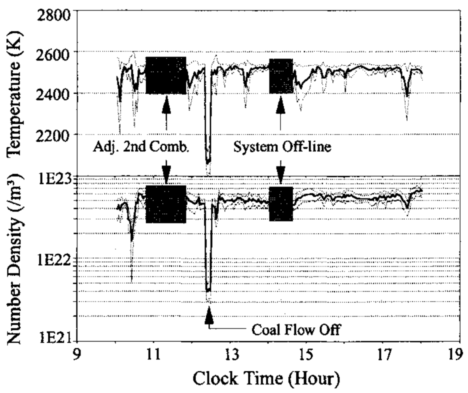

Fig. 8 Measurements of temperature and potassium atom number density in the aerodynamic duct of the CFFF for the LMF5-G test.

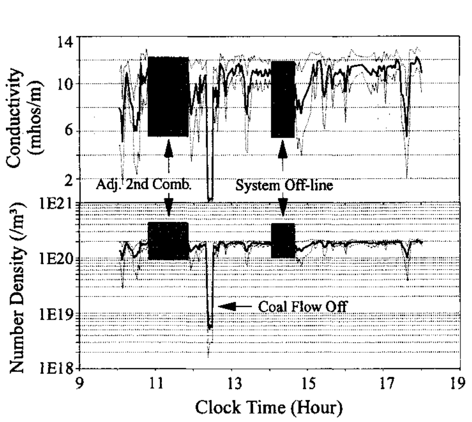

Fig. 9 Measurements of electron number density and conductivity in the aerodynamic duct of the CFF for the LMF5-G test.

At the aerodynamic duct the flow velocity is quite high (>1 km/s), and the high potassium density measurement standard deviation was believed to be due to the noncoincidence of the exposures for the two separate signals, i.e., flame-emission and lamp transmission. Therefore, for later experiments the single beam optics were replaced with a two-beam optical arrangement for spatially separate, but temporally coincident signal collection as shown in Fig. 7. A single optical chopper with a 5-deg opening was used with the two fibers—each signal is an 0.5-ms exposure corresponding to a view of 50 cm or more of flow at a velocity of greater than 1 km/s. Considerable reductions in the measurement uncertainties were found with this new signal collection scheme as seen in Fig. 8.

The beam diameters at the crossing in the center of the flow are about 1 cm, so the beams are essentially overlapped while traveling inside the flow volume, especially considering that the signals average light from about 50 cm of flow during the 0.5-ms exposures. A major possible source of systematic error is the scattering by ash/slag particle of lamp light into the flame-only beam. At the elevated temperatures of the aerodynamic duct, the particle loading is expected to be low and scattering is not expected to be a problem. This is confirmed by the low frequency of Doppler bursts recorded by the LDV system at this location.[13]

The two-beam optical scheme provides a standard deviation for the potassium number density of about 20%, a considerable reduction from the 50–100% for the temporal separation scheme, approaching the limits for a stable bench-top flame. The excellent agreement in average measured potassium density for the two schemes on different tests—but with the same nominal conditions—indicates that the temporal separation scheme does provide valid measurements in spite of the noise.

Figure 9 shows that with the lower standard deviations for temperature and potassium density, reasonable results are found for calculating the electron density and electron conductivity. These results were found using an estimated pressure of 1.78 atm. The calculations of electron conductivity are especially sensitive to any errors in pressure, so without a pressure measurement concurrent with the emission absorption measurements, the conductivity calculation can only be considered a rough estimate.

Discussion

For a confined turbulent flame, the physical dimension of local equilibrium is limited by (not necessarily equal to) the smallest confinement size. Suppose that the smallest confinement dimension is d and the speed of the flow is v, then the time for a section of local equilibrium to fly by is less than d/v. This time is the upper limit allowed for collection of the flame emission and transmitted lamp signals in order to ensure that a temporal separation optical scheme will be valid.

At the CFFF diffuser, the flow diameter is 76 cm and LDV measurements at the exit of the diffuser of the CFFF show the flow speed to be less than 100 m/s.[14] Thus, the minimum local equilibrium characteristic time is about 7.6 ms, which is well outside the 1-ms signal collection delay for the temporal separation scheme. The 1-ms delay between the flame emission signal and the lamp plus flame signal is clearly not a problem for this location.

In contrast, at the aerodynamic duct the flow diameter is 12 cm and the average flow speed is approximately 1000 m/s, thus the minimum estimate of local equilibrium time is about 0.12 ms. Also, the flame is expected to be more turbulent at the aerodynamic duct than at the diffuser, and considerable fluctuations in the flow parameters could and would be expected to occur during a 1-ms signal collection delay at the aerodynamic duct.

The two-beam, spatially separated optical scheme improved the measurements considerably, but not without tradeoffs. This optical setup requires greater optical access and an additional optical fiber, is more difficult to align, and the alignment is more difficult to maintain on a large-scale facility with significant vibrations because of the low f number of the collimating lenses. However, the results clearly indicate that the coincident, spatially separate signal collection scheme is the solution for measurement in high-speed, turbulent flows.

Acknowledgments

This work was sponsored by the Department of Energy, Contract DE-AC02-80ET15601.

References

[1]Cook, R. L., et al., "Overview of Recent Diagnostic Measurements at the USA MHD Facilities," *Proceedings of the 11th International Conference on Magnetohydrodynamic Electrical Power Generation*, International Academic Publishers, Beijing, China, 1992, pp. 953–964.

[2]Cook, R. L., and Lineberry, J. T., "Design and Evaluation of an Optical Port Assembly for the Aerodynamic Duct at the CFFF," *Proceedings of the 30th Symposium on Engineering Aspects of MHD* (Baltimore, MD), Seam, Inc., Tullahoma, TN, 1992, pp. XIII.1.1–9.

[3]Bauman, L. E., "Investigation of MHD Flow Structure and Fluctuations by Potassium Lineshape Fitting," *Proceedings of the 31st Symposium on Engineering Aspects of MHD* (Whitefish, MT), Seam, Inc., Tullahoma, TN, 1993, pp. X.5.1–15.

[4]Jeanmaire, P., "Application of Line Reversal Method to Measurement of Shock Flow Electron Temperature," *Physics of Fluids*, Vol. 17, No. 2, 1974, pp. 353–359.

[5]Kayukawa, N., Aoki, Y., and Ozawa, Y., "Application of Light Polarization Technique to the Generalized Line-Reversal Method for Gaseous Temperature Measurements," *Review of Scientific Instruments*, Vol. 53, No. 11, 1982, pp. 1653–1656.

[6]Winkelman, B. C., Giel, T. V., and Baucum, W. E., "Temperature and Spectral Emission/Transmission Measurements in the DOE Coal-Fired Flow Facility," *Proceedings of the 21st Symposium on Engineering Aspects of MHD* (Argonne, IL), Seam, Inc., Tullahoma, TN, 1983, pp. 8.7.1–11.

[7]Bauman, L. E., and Wolverton, M. K., "Time-Resolved Line Reversal Gas Temperature Measurements Using a Multi-Channel Detector," *Proceedings of the 9th International Conference on MHD Electrical Power Generation* (Tsukuba, Ibaraki, Japan), International Liaison Group on MHD Electrical Power Generation, Yokohama, Japan, 1986, pp. 563–572.

[8]Onda, K., Kaga, Y., and Kato, K., "Measurement of MHD Combustion-Gas Temperatures and Potassium Number Densities in the Presence of Cold Boundary Layers," *Journal of Quantitative Spectroscopy and Radiative Transfer*, Vol. 26, No. 2, 1981, pp. 147–156.

[9]Bauman, L. E., Luthe, J. C., and Ma, X., "An Emission Absorption Technique Suitable for Automatic Measurement of Seed Atom Density in Coal Fired MHD Flows," *Magnetohydrodynamics: An International Journal*, Vol. 3, Nos. 1/2, 1992, pp. 43–53.

[10]Bauman, L. E., "Bias and Uncertainty in Emission Absorption Measurements of Temperature and Atomic Number Density," *Journal of Thermophysics and Heat Transfer*, Vol. 6, No. 4, 1992, pp. 746–752.

[11]Bauman, L. E., "Potassium D-Line Blue Wing Absorption Coefficient Under Combustion-Fired MHD Conditions," *Journal of Thermophysics and Heat Transfer*, Vol. 7, No. 1, 1993, pp. 25–29.

[12]Frost, L. S., "Conductivity of Seeded Atmospheric Pressure Plasmas," *Journal of Applied Physics*, Vol. 32, No. 10, 1961, pp. 2029–2036.

[13]Wilson, W. W., Singh, J. P., Yueh, F. Y., George, A., Cook, R. L., and Lineberry, J. T., "Comparison of Velocity and Temperature Measurements in the CFFF Aerodynamic Duct with Flow Field Model Calculations," *Proceedings of the 31st Symposium on Engineering Aspects of MHD* (Whitefish, MT), Seam, Inc., Tullahoma, TN, 1993, pp. X.5.1–15.

[14]Wilson, W. W., Srikantaiah, D. V., Lineberry, J. T., and Lee, J. J., "Comparisons of LDV Results with Theoretical Flow Predictions for the CFFF Radiant Furnace," *Proceedings of the 27th Symposium on Engineering Aspects of MHD* (Reno, NV), Seam, Inc., Tullahoma, TN, 1989, pp. 3.4-1–12.